Sensing and Bio-Sensing Research 29 (2020) 100368

Contents lists available at ScienceDirect

Sensing and Bio-Sensing Research

journal homepage: www.elsevier.com/locate/sbsr

Nanocellulose- based biosensor for colorimetric detection of glucose

Katrin Neubauerova[a,c,1], Mariana C.C.G. Carneiro[a,b,d,1], Lígia R. Rodrigues[d], Felismina T.C. Moreira[a,b,d,*], M. Goreti F. Sales[a,b,d]

[a] BioMark/ISEP, School of Engineering, Polytechnic of Porto, Porto, Portugal
[b] BioMark/UC, Department of Chemical Engineering, Faculty of Sciences and Technology, University of Coimbra, Coimbra, Portugal
[c] Laboratory of Bioengineering and Functional Materials, University of Chemistry and Technology, Prague, Czech Republic
[d] CEB - Centre of Biological Engineering, University of Minho, Campus de Gualtar, 4710-057 Braga, Portugal

ARTICLE INFO

Keywords:
Nanocellulose
TEMPO-based oxidation
Glucose oxidase
Colorimetric
Test-strip
Biosensor

ABSTRACT

This work reports for the first time a colorimetric based biosensor using nanocellulose (NC) based supports drop-deposited onto a cellulose paper substrate for glucose detection in point-of-care. For this purpose, micro-crystalline cellulose (MCC) samples were oxidized with 2,2,6,6-tetramethylpiperidine-*N*-oxyl radical (TEMPO), sodium hypochlorite, and potassium bromide, to produce carboxylated NC. For the characterization, we used several methods: TEM, FTIR and conductometric titration. In all samples, the primary alcohol groups were selectively oxidized into carboxyl groups, provided the sodium hypochlorite is added dropwise and the reaction is performed at constant pH 10. Carboxyl- NC was further casted on a cellulose substrate and used as support for glucose oxidase (GOx), horseradish peroxidase (HRP) and 2,2′-Azino-bis(3-ethylbenzothiazoline-6-sulfonic acid) diammonium salt (ABTS) reactions, aiming to yield a coloured detection system for glucose.

The sensing system was generated by integrating GOx on the carboxyl- NC /cellulose substrate. Upon reaction with glucose, the enzyme produced hydrogen peroxide, which was converted into a blue-coloured product by reaction with HRP and the chromogenic reagent ABTS. The test-strip was calibrated by incubating it in different concentrations of glucose. The colours obtained were further analysed by a suitable image analysis software. Linear response for glucose ranged from 1.5 to 13.0 mM.

Overall, this new test-strip used renewable material for glucose determination, which is an advantage when compared to other systems that require more complex technological approaches. Moreover, it was found that carboxyl- NC improved the colour homogeneity of the test-strip and the intrinsic linear response of concentration range.

1. Introduction

Cellulose is one of the most abundant biopolymers produced on earth. It offers excellent renewability, recyclability and biodegradability features [1–3]. It is a long linear homopolymer polysaccharide structure combining D-glucopyranose units linked through β(1–4) glycosidic bonds. Its chemical modification, such as esterification, etherification, silylation, or polymer grafting reactions, is widely involved to produce material with different chemical moieties or structures. [2,4,5].

Nanocellulose (NC) materials are among the different products that may be obtained from cellulose by combining proper mechanical, chemical, and enzymatic treatments [6]. They display outstanding properties, such as high surface area, mechanical strength, high thermal and chemical durability or film-forming capacity [7–9]. NC have a highly crystalline structure, with a rod-like shape ranging 2–50 nm width and 100–2000 nm length [10,11].

The most popular process for producing NC is acidic hydrolysis [12], employing typically concentrated sulphuric acid [13,14] and/or hydrochloric acid [15,16]. In sulphuric acid-based hydrolysis, sulphate ester groups are introduced on the surface of the NC. This leads to the formation of highly stable NC suspensions, because negatively charged sulphate groups are attached to the surface of the NC. However, sulphuric acid is strongly oxidizing, and sometimes causes the degradation of cellulose. Unlike sulphuric acid hydrolysis, hydrochloric acid hydrolysis yields.

The TEMPO-mediated oxidation is an alternative promising procedure, which can produce nanocrystals with modified surface in one

* Corresponding author at: School of Engineering of the Polytechnic School of Porto, R. Dr. António Bernardino de Almeida, 431, 4249-015 Porto, Portugal.
E-mail address: ftm@isep.ipp.pt (F.T.C. Moreira).
[1] Katrin Neubaueriva and Mariana Carneiro share equal first author

https://doi.org/10.1016/j.sbsr.2020.100368
Received 27 April 2020; Received in revised form 3 July 2020; Accepted 10 July 2020

step. TEMPO radicals catalyze oxidation of hydroxyl groups and after system supported by NaClO-KBr components converts oxidized aldehydes into final charged carboxyl groups [17–19]. The use of this technique was attracting by many investigations since 1994, showing that only the primary alcohol groups of polysaccharides were oxidized, whereas the secondary hydroxyls remained unaffected [20].

For cellulose, the TEMPO-mediated oxidation was applied to different types of cellulose, ranging from cotton, to wood pulp, cell cellulose, rayon and cellulose III [16,21–25]. These studies led to the preparation of a series of products, ranging from water-soluble polyuronic acid to partially derivatized cellulose products.

According to previous results [17,18], TEMPO-mediated oxidation was applied to microcrystalline cellulose (MCC) and a pretreatment method of first oxidation was devised to prepare water-soluble polyuronic acid in a high yield, which was dependent on the reaction temperature during first and second oxidation. In literature [4], the relationships between the amount of NaClO was optimized and either carboxylate or aldehyde content in oxidated NC. The carboxyl group content increased remarkably to 0.68 mmol/g solid with the addition of at least 5 mmol of NaClO/g MCC. The oxidation of primary alcohol groups in cellulose, catalyzed by TEMPO, has been recently proposed as a more selective, faster, and better-controlled method. [2,5].

Due to its remarkable characteristics, NC is one of the most attractive cellulose-based nanomaterial used in biosensors and biomaterials applications. [26–29]. Cellulose and NC have been widely used as a support material for proteins/enzymes immobilization [3,5,30–36], making use of optical or electrical transduction schemes [1,6,27,37–39], due its outstanding characteristics of these materials. Besides, specially NC shows a high surface area promoting an easy analyte immobilization [6].

Several lateral flow assays (LFAs) have been widely used for glucose analysis in urine [40]. However, this procedure is rather complex, because it uses a porous membrane with specific antibodies or proteins immobilized in lines [41]. Besides, LFAs show other concerns, as it is based in a “one-step” assay, in which the sensory surface is not easily washed and, consequently, may suffer from interference of sample components that pre-block the strips. Beyond that, these assays demonstrate a qualitative and semi-quantitative nature [40]. In addition, sometimes it is necessary to label the antibody in order to increase the sensitivity, losing the one-step concept, becoming a more complicated and expensive assay, especially accounting the needs of a very selective antibody.

A similar tool to LFA using cellulose as a support material is the well-known dipstick based sensing system [42]. When the dipstick gets in touch with the sample (urine or other physiological fluid), a colour change in the stick is generated. [39,42–44]. This method is simple but it offers a response of semi-quantitative nature, thereby limiting the accuracy of the analytical data generated.

Some biorecognition elements were also employed in paper-based biosensors, including enzymes [45]. Enzymatic biosensors use enzymes as a biological recognition element [46–50] and offer highly selective responses. In the case of preparing of enzyme-based biosensor, it is essential to ensure that enzymes are available to catalyze the intended reaction and must be stable under the normal reaction conditions of the biosensor [47,48]. Several enzymatic assays, with different enzymes immobilized on the cellulose paper surface aiming to detect different analytes, have been reported in the literature. These include glucose [45], lactate [51], stearate [52], catechol [53], phenol [54], among others.

The main issue concerning the preparation of enzymatic based-cellulose sensors is related to the enzyme immobilization on paper substrates. Several techniques have been reported in the literature for this purpose [55], mainly based on adsorption [56] and covalent attachment [57,58]. Adsorption is a simple methodology but hinders the typical binding capacity of enzymes for being immobilized randomly on a solid cellulose support. In addition, the enzymes are sensitive to harsh conditions as pH and temperature, leading to some concerns in terms of sensor reliability. Other methodologies include chemical cross-linking [59], thin film entrapment [55], and microencapsulation [60]. These increase the effectiveness of enzyme immobilization but may limit the accessibility of the substrate and increase the complexity of the assay development and associated costs.

This work combines the TEMPO-oxidation of MCC to produce carboxyl-NC and their application in the development of colorimetric based test-strips for glucose. The MCC oxidation is optimized, as well as the integration of the GOx within the cellulose/-NC-based substrate, and the ability to generate colour in the presence of H_2O_2. Overall, this works reports for the first time the integration of -NC with enzymatic biosensor, for glucose detection in urine samples in diabetes.

2. Experimental methods

2.1. Materials

Microcrystalline cellulose was obtained from Biochem Chemopharma. TEMPO (2,2,6,6-tetramethyl piperidine-1-oxyl radical), ABTS (2,2′-azino-bis(3-ethylbenzthiazoline-6-sulphonic acid), 98%), EDC (3-(ethyliminomethyleneamino)-*N,N*-dimethylpropan-1-amine, 99%), MES monohydrate (2-(*N*-morpholino)ethanesulfonic acid monohydrate, $C_6H_{13}NO_4S{\cdot}H_2O$, 99%) and Glucose Oxidase HPS 300, activity 260.3 U/mg from SCKISUI and uric acid were supplied by Sigma Aldrich. Sodium hydrogen carbonate ($NaHCO_3$, > 99%), sodium chloride (NaCl), hydrochloric acid (0.5 M) and hydrochloric acid (37%) were purchased from Panreac. Sodium hypochlorite solution (NaClO, ca. 10% active chlorine, 15% solution) was obtained from Carlo Erba, sodium carbonate (Na_2CO_3) and L-ascorbic acid were supplied by Riedel-de-Haen. Glucose (dextrose monohydrate, $C_6H_{12}O_6{\cdot}H_2O$) Alfa Aesar. Sodium hydroxide (NaOH, solid pellets) was purchased from Eka. NHS (N-hydroxysuccinimide, > 97%), HRP (horseradish peroxidase, 150 U/g) and creatinine were obtained from Fluka. Urea was supplied by Fragon. Ethanol (96%) was purchased from José Manuel Gomes dos Santos. Phosphate Buffered Saline (PBS) tablets were obtained from Amresco, dissolved in Mili-Q water and pH was changed to 7.2. Purified Milli-Q water was used for all the experiments and analysis. All chemicals were used without any prior purification.

2.2. Pre-treatment of MCC

MCC was pre-treated according to literature [18]. Two different protocols were used for this purpose: 1 g of MCC was added to 13 ml of HCl (37%), stirred and hydrolyzed at 45 °C for 30 min or 1 g of MCC added to 10 ml of HCl (37%) and hydrolyzed at 100 °C for 15 min. After the acidic hydrolysis, the dispersion was washed and centrifuged three times, at 12000 rpm. The final wash was made in a dialysis membrane with distilled water, until neutral pH was reached. The solution containing the supernatant was sonicated for 15 min, in order to obtain NC. The MCC residue obtained was filtered. NC was precipitated in ethanol, filtered and dried in oven at 60 °C.

2.3. Tempo-oxidation of nanocrystals

TEMPO-mediated experiments were carried out as previously published with minor modifications [17] and the pictures of the resulting materials at intermediate stages are shown in Fig. 1. The first oxidation was made by dispersing 1 g of MCC in carbonate buffer solution (75 ml, pH = 10.83), in a sonicator (15 min), and adding TEMPO (30 mg) and KBr (0.32 g) into this suspension, maintained at 30 °C. The sodium hypochlorite solution (15%, 6 mL) was then added to the resulting suspension, which was mechanically stirred. The pH was kept at 10, in order to prevent a severe degradation of the water-soluble polymer. After stirring for 5 h, the reaction was terminated by adding 20 ml of ethanol, which reacted with the remaining TEMPO. The reaction

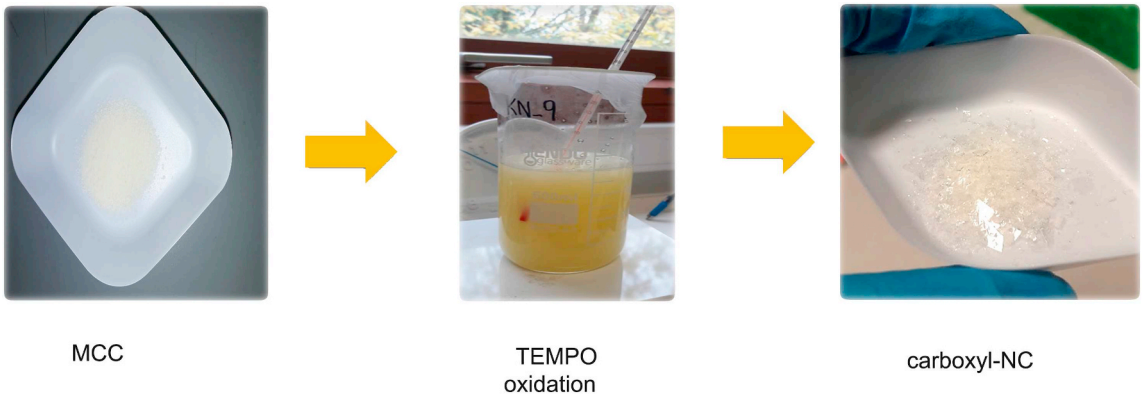

Fig. 1. Synthesis of the carboxyl-NC by TEMPO oxidation of MCC.

mixture was acidified to pH 3 (for removing K^+ cations) with 0.5 M HCl, and centrifuged to remove the residual insoluble microcrystalline material. The water-soluble NC in the supernatant were precipitated by adding an excess of ethanol (up to 400 ml), followed by centrifugation. The precipitate was washed with ethanol, centrifuged several times and finally dried in the oven, at 45 °C. The residual MCC was washed with ethanol and also dried at 45 °C in the oven, acting as the raw material for the next oxidations. The second and the third oxidation procedures consisted in repeating the previous experiments.

2.4. Nanomaterial characterization

2.4.1. Conductometry

The carboxyl content of oxidized nanocellulose samples was determined by conductometric titration [17]. Dried nanocellulose samples (30–40 mg) were resuspended in 15 mL of 0.01 M HCl solution. After 10 min of sonication and stirring, the suspension was titrated with 0.01 M NaOH. According to [17], the content of carboxyl groups in the material was expressed in the form of degree of oxidation (DO), as given by the following equation,

$$DO = \frac{162 \text{ x } C \text{ x } (V_2 - V_1)}{w - 36 \text{ x } C \text{ x } (V_2 - V_1)} \quad (1)$$

where V_1 and V_2 are the amount of NaOH (in L), c is the NaOH concentration (mol/L), and w is the weight of dried sample (g). The value of 36 corresponds to the difference between the molecular weight of an AGU and that of the sodium salt of a glucuronic acid moiety.

2.4.2. Fourier-transform infrared spectroscopy

The NC and the MCC were analysed via FTIR spectroscopy to evaluate the chemical modifications. The resulting spectra were used to determine the structural characteristics of the nanocellulose.

Infrared spectra were recorded on a FTIR Thermo Scientific spectrometer (Nicolet iS10) with an ATR (attenuated total reflectance) accessory, having a diamond crystal. Spectra were analysed from 400 to 4000 cm^{-1} wavenumber, with a 2 cm^{-1} resolution, and an accumulation of 150 scans, after background collection.

2.4.3. Transmission electron microscopy

Dried oxidized NC was dissolved in water (0.01% w/v) and sonicated for 15 min. A drop of this suspension was deposited on the electron microscope grid and negatively stained with phospho-tungstic acid for 10 s. The excess of liquid was removed by a filter paper. The grids were observed in a TEM Zeiss, Model EM902 A.

2.5. Colorimetric assay

2.5.1. Binding of glucose oxidase to the NC

2.5.1.1. Glucose oxidase (GOx) adsorption. An oxidized carboxyl-NC (20 mg) was dispersed in 10 ml of 50 mM MES buffer with 500 mM NaCl buffer (pH 5.0) and kept stirring for 24 h at room temperature, before use. Then, 2.5 μL of carboxyl-cellulose was casted on the cellulose surface. After, a solution of GOx (2.0 mg/mL) previously dissolved in PBS buffer, was drop-casted on the modified cellulose paper with the NCs. The sensors were let to dry at room temperature and stored in the fridge at 4 °C before use.

2.5.1.2. Covalent attachment of GOx. The carboxyl groups of the carboxyl-NC were activated using EDC/NHS. 12 mg of NHS (10 mM) and 8 mg of EDC (4 mM) were added into the well-dispersed mixture of carboxyl-NC (20 mg) in 10 ml of 50 mM MES and 500 mM NaCl buffer (pH 5). The solution was stirred for 24 h at room temperature. The excess of reactants was removed by precipitating of the activated carboxyl-NC in ethanol. The precipitate was centrifuged, cleaned with ethanol and oven-dried to eliminate ethanol residues. The activated material was dispersed in 12 mL of PBS (pH = 7.2) containing 20 mg of GOx. This dispersion was stirred 24 h at room temperature. Then, 2.5 μL of the previous solution was drop-casted in the cellulose paper.

2.5.2. Colorimetric assay

2.5.2.1. Carboxyl-NC and glucose oxidase concentration optimization. For glucose detection, oxidized- NC (0.01–20 mg/mL 2.5 μL) was adsorbed on a cellulose paper substrate. The next stage consisted of the immobilization of GOx. The concentration of the enzyme was studied within 0.001 and 0.5 mg/mL, by using 2.5 μL of the enzyme solution. For this purpose, the enzyme was casted on the cellulose/carboxyl-NC surface and let to dry at room temperature. Then, 22.5 μL of a solution consisting of different concentration of glucose i(0.001 to 100 mM, 1.2 μL), PBS (pH 7.2, 18.9 μL), ABTS (5 mM, 1.2 μL) and HRP (150 U/g solid, 1.2 μL), was dropped on the filter paper substrate with, containing the carboxyl-NC [61] (Fig. 2A). The colour of each test-strip was monitored for periods of 3, 5 and 10 min of incubation. Resulting colour was compared with colour of the blank sample containing only glucose without enzyme.

Pictures of the results were obtained by smartphone camera. However, light conditions highly influence quality and reproducibility of the acquired images and the feasibility of results.Thus the pictures were taken in controlled light conditions and a fixed focal distance.

Image J software version 1.4.3.67 have been used to analyse the results. A square tool have been used to select a constant area for the measurements. Several parameters were analysed as RGB (red, green and blue). The average of (red, green and blue) channel image provided the best results in terms of linearity when plotted against glucose concentration and was used for analysis.

2.5.3. Selectivity assay

The selectivity of the system is a crucial parameter for the analysing system when it is expected to be applied under real conditions. For this

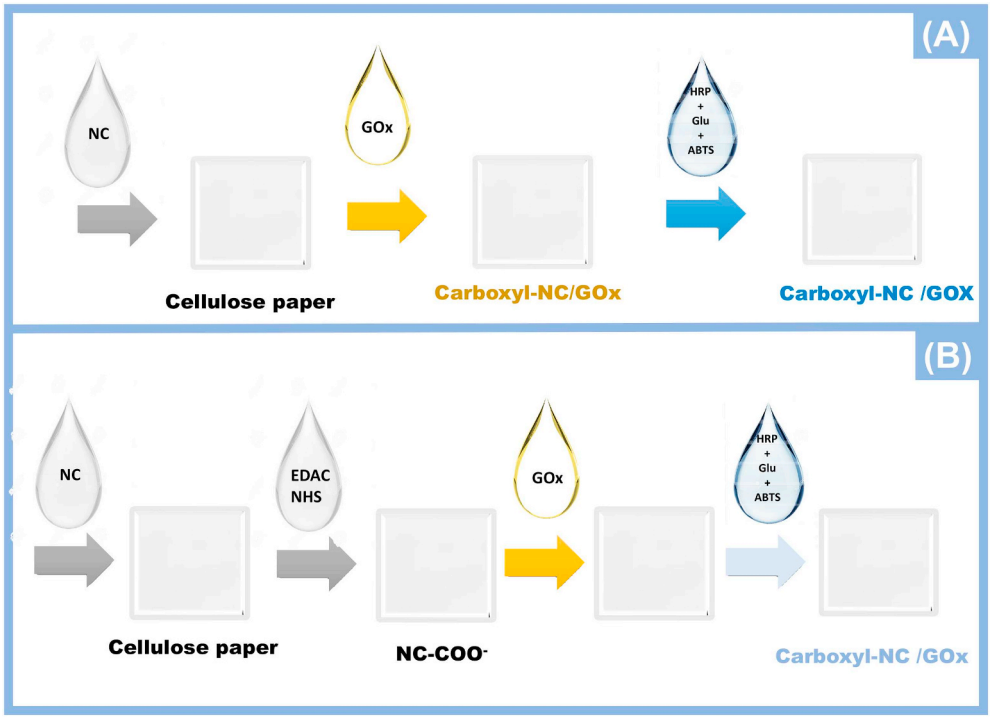

Fig. 2. Test-strip based colorimetric assay produced by casting on the cellulose substrates the indicated solutions, and binding GOx either by adsorption (A) or by covalent bonding (B).

reason, the selectivity of the sensing system was further evaluated by incubating different interfering molecules, present in urine samples, onto the test-strips. Glucose (19.2 mM) plus ascorbic acid (0.01 M), glucose (19.2 mM) plus acid uric (0.06 mg/mL), glucose (19.2 mM) plus creatinine (12 mM) and glucose (19.2 mM) plus urea (0.2 mg/mL). Assays were prepared in PBS and dropped on the filter paper as previously described at "2.5.2 Assay for detection of glucose". Images of the results were captured and ImageJ was used to obtain the parameter values and calculate the errors.

3. Results and discussion

3.1. The oxidation of MCC

The oxidation of raw cellulose by means of the TEMPO reaction is often incomplete. On the other hand, pre-treated cellulose can give larger amount of totally oxidized water-soluble polyglucuronans [18]. Thus, the oxidation of MCC by TEMPO reaction may be more effective by establishing sequential oxidative reactions. In general, at least two oxidation stages were applied herein, in which the oxidized material was removed from the solution and the remainig MCC material was further subjected to a second oxidation stage. A third oxidation was also processed to show if this would enhance the oxidative yield or the properties of the final material.

Herein, MCC was oxidized with sodium hypochlorite, combining catalytic amounts of potassium bromide and TEMPO radicals, under various conditions, as described in Table S1. The effect of the number of sequential oxidative procedures, and the concentration/volume of sodium hypochlorite, on the NC weight yield was tested by using four different samples, named A to D (Table S1). Sample A was prepared according to the procedure described in [18], by using 13.4 mmol of hypochlorite per gram of MCC. The weight yield in the first round of oxidation was reasonable (13%), but in the second round it decreased to only 3%. The efficiency of the oxidation of MCC into NC was further optimized by using a higher concentration of hypochlorite (24 mmol of hypochlorite per gram of MCC), added at once or in multiple times. In sample B, the whole volume of hypochlorite was added at the beginning of the each oxidation reaction. Comparing to sample A, the weight yield in the first oxidation was similar, but the second oxidation provided higher yields (5 times more, equal to 15%) and from the third oxidation was obtained 11% yield. In samples C and D, the same volume of hypochlorite was added sequentially, divided in three and six times, respectively. Comparing single and multiple addition of hypochlorite, the effect was evident. The NC yields in all the 3-round oxidations significantly increased by adding a smaller amount in multiple times. Overall, the best results were obtained for samples C and D, corresponding to the highest yields in all oxidations of MCC. Procedure of sample D provided most oxidized material.

It is obvious that the efficiency of the MCC oxidation using the TEMPO-NaClO-KBr system to produce water-soluble NC depends positively on the increasing amount of hypochlorite, up to a limiting value when the cellulose structure would be fully destructed. Moreover, multiple addition of the smaller volume of reagent into the solution provides higher yield, because there is more fresh reagent capable of starting new oxidative reactions. After these results, subsequent studies used sample D as a support material for the enzyme immobilization.

3.2. Characterization of the materials

3.2.1. Fourier-transform infrared spectroscopy

TEMPO-oxidation reaction of primary alcohol groups was evaluated by FTIR spectroscopy, searching for the presence of carbonyl or carboxyl acid functional groups. The infrared spectra of initial raw MCC and carboxyl- NC are shown in Fig. S1.

Overall, the FTIR spectra of pristine MCC contains a strong peak around 3500 cm^{-1} region, attributed to the O—H stretch of cellulose. This peak was an indicator of high concentration of alcohol groups (ROH) in cellulose. The strong peak at 1060 cm^{-1} was assigned to the stretching of the C—O bond in the cyclic structure of glucose. This band is related to groups of secondary alcohols and secondary ethers [62].

After TEMPO oxidation, a new relevant peak appeared at 1730.9 cm^{-1}. It corresponded to the C=O stretching vibration of

carboxyl groups in their acidic form. Consistently, the peak at 1611.2 cm^{-1} was assigned to the presence of anionic forms of carboxylic acids. Moreover, the peak was signalling the stretching vibration of C—O shifted to a higher wavenumber (herein 1037.1 cm^{-1}), as expected. Finally, the stretching vibration of C—H at 2896 cm^{-1} was of lower intensity and the band at 3333 cm^{-1} was broader, also signalling the presence of the carboxylic acid groups.

When compared to the pristine MCC, the combination of these peak changes in the FTIR spectra confirmed the oxidation of primary hydroxyl groups by TEMPO [4,5,17–19], leading to the formation of carboxyl- NC. Overall, peaks in obtained spectra demostrated that some hydroxyl groups of the D-glucose cyclic unit were converted into carbonyl groups successfully, leading to the formation of carboxylic or aldehyde groups..

3.2.2. Conductometric assay

The carboxylic content in the oxidized NC was evaluated by acid/base conductometric titration. As shown in Fig. S2.There are three stages of conductivity that are also described, in the literature [17–19]. First, a decrease of conductivity was observed, which revealed the titration of the excess of HCl present in the solution. The concentration of H^+ decreased because reaction with HO^- resulted in forming water (a non-ionic specie that cannot change the conductivity of the titrated solution), and the concentration of Na^+ increased (due to the increasing addition of NaOH). As H^+ has a higher intrinsic conductivity than Na^+, the conductivity signal dropped with the increasing NaOH concentration, until a minimum value at which the strong acid was consumed. This minimum value was V_1 in Eq. (1). The second stage of this titration was signalled by a more or less steady conductivity signal against the addition of NaOH, and corresponded to the titration of the carboxylic acid groups. Then the HO^- was being added leading to shifting the H^+ from the carboxylic groups to form water, also leading to the formation of the corresponding conjugated base that had an anionic form ($-COO^-$). Thus, the concentration of H^+ was decreasingand the signal should be decreasing as well. However, this was being compensated by an increasing amount in both Na^+ and $-COO^-$, justifying that no significant variation was observed. The end of the carboxylic group titration signalled V_2 in Eq. (1). The third stage of the calibration started after V_2. Only increasing amount of added Na^+ and HO^- increased the conductivity, because all acids in the solution had been neutralized before and there was no acid/base reaction taking place.

Considering all titrations, the results pointed out that the water-soluble cellulose oxidized samples had approximately 0.7 to 0.8 mmol/g of carboxylic content. The results were reproducible among samples and they did not seem to be influenced by the different optimization of processes considering samples D. From these, it was assumed that the average degree of oxidation was 15%, which was a considerable level of oxidation decribed in the current literature.

3.2.3. Transmission electron microscopy

The morphological analysis of all samples was made by TEM, in which the presence of *nanowhiskers* in the solution was confirmed. Fig. 3 indicates that there is a large poly-dispersity in the distribution of both the length and the width of the whiskers. Indeed, their length ranged from around 50 nm to more than 300 nm, with an average size of 100 nm. Regarding their width, valued from 5 to 20 nm were measured, but most of them are close to 20 nm.

Overall, the size and the structure obtained herein are in agreement with the literature [63,64], in which Nie et al. also reported the presence of CNC after TEMPO oxidation. They obtained a similar nanowiskers, in terms of shape and size, with about 250–300 nm long and 10–20 nm width [64].

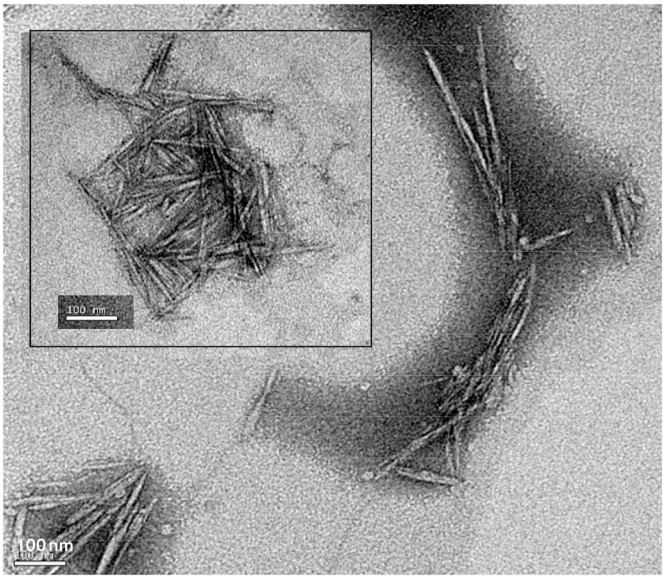

Fig. 3. TEM images of carboxyl- NC material obtained after TEMPO oxidation of MCC.

3.3. Glucose sensing system

The use of carboxyl- NC material as a suitable support for a sensing system was tested herein using the conventional glucose enzymatic-based assay. Briefly, glucose was used as substrate, GOx acted as the enzyme that catalyses the selective oxidation of glucose, and peroxidase (HRP) and ABTS were employed colorimetric system for the detection of the products that signalled indirectly the oxidation of glucose. Overall, this is a well-known reaction and is employed herein to develop a test-strip for glucose.

3.3.1. GOx concentration study

GOx (2 mg/mL) was prepared in PBS buffer solution and drop-casted (2.5 μL) on a filter paper surface and let dry at room temperature. The enzymatic response was observed against different concentrations of glucose (22.5 μL), ranging from 0.1 to 10 mg/mL, previously prepared in PBS buffer pH 7.4. The results obtained under the

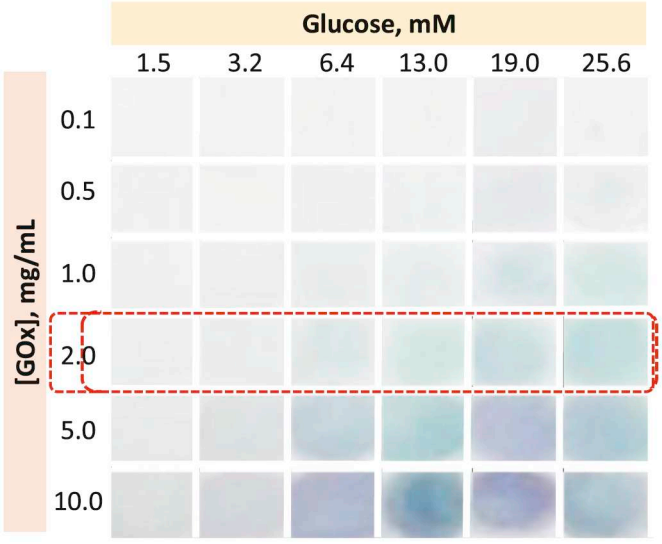

Fig. 4. Digital images of the calibration curves of glucose using GOx test-strip adsorbed to the test-strip.

different glucose oxidase concentration are shown in Fig. 4. In these, each GOx concentration was tested against glucose concentrations ranging from 1.5 to 25.6 mM.

In general, it was obvious that higher concentrations of glucose and higher concentrations of GOx yielded more intense blue colours, which was expected. However, considering the purpose of designing a test-strip, it was also important that the colour change occurred in a gradient format. This gradient meant that the absorption of GOx into the support was more reproducible, thereby ensuring more reliable analytical data. In terms of gradient colour change against the concentration, this was more evident when 2.0 mg/mL of GOx (260.3 U/mL) were being used, and therefore this concentration was selected for further studies.

3.3.2. *Time effect*

Considering that the reaction is of enzymatic-nature, it was very important to monitor the colour of the test-strip within time. In general, as enzymatic reactions are quick, the colours on the test-strip appeared immediately after dropping of reagents on the material and these were evolving fast within time. After 6 min, most of test-strips turned dark purple, depending on the concentration of glucose and GOx. For the higher concentrations of glucose and GOx, the purple colour on the paper was observed since the very first moments, indicating that the reaction reached its maximum extent under that conditions. Therefore, the reaction was performed and observed at different time intervals. According to obtained results, the ideal time for analysing the colours ranged from 3 to 5 min since the beginning of the reaction. A period of 3 min was set for the subsequent tests, allowing a shorter period of reaction and leading to suitable detectability features (Fig. S3).

3.3.3. *Sensing system bound by adsorption to the oxidized NC*

While the chemical system for glucose detection is well-known, information about the effect of the carboxyl- NC on the colour gradients or concentration ranges of detection is missing. In general, it was expected that the presence of carboxylate groups on a cellulose substrate would enhance its binding efficiency and create a suitable environment for GOx activity. In terms of binding efficiency, a regular cellulose substrate would establish interactions with GOx via hydrogen bridges only. When cellulose is doped with carboxyl- NC these interactions could be enhanced by the presence of multiple −COOH groups, which would intensify the hydrogen bridges and establish ionic interactions with multiple positive points existing in the external surface of GOx. Thus, different tests-trips were prepared by casting different amounts of NC-COOH on the cellulose substrate, ranging from 0.010 to 20 mg/mL and let to dry after casting. These studies were made by keeping the previously defined concentrations, having 2.0 mg/mL GOx and 3 min for the reaction to take place. Fig. 5 summarizes the results obtained from different concentrations of glucose, ranging from 1.5 to 25.6 mM.

When compared to the results obtained without carboxyl- NC the observed colours were more homogenously distributed along the whole surface of the test-strip and the gradient colour change was improved by the presence of the carboxylated- NC. Overall, this confirmed that the presence of carboxyl- NC affected positively the results obtained by improving the colour features of the glucose detection.

However, there was not a great difference among the different test-strips prepared with increasing amounts of carboxyl- NC. This was probably linked to the saturation of carboxyl- NC adsorbed on the cellulose support for the selected concentration range. Thus, an intermedium concentration of 5 mg/mL was selected for subsequent studies, considering reproducibility and cost purposes. This would ensure highly reproducible strips at a lower cost than those employing the highest concentration tested.

Comparing the analytical performance of test-strips prepared without carboxyl- NC and with 5 mg/mL carboxyl- NC a linear trend was observed in both by plotting (R + G + B)/3 against glucose concentration. The presence of carboxyl- NC yielded improvements in terms of lower limit of linear range, decreasing the observed value from 6.4 to 1.5 mM. Moreover, the slope increased about 50% by the presence of carboxyl-NC, increasing the slope value from 1.0 to 1.5 a.u/mM. Additionally, the operational features in terms of lower limit of linear demonstrated improvements starting 1.5 mM with NC and 6.4 mM for the biosensor without NC.

Overall, these results confirmed that the loading of GOx on the test-strips and its catalytic activity were more controlled by the presence of carboxyl- NC.

3.4. *Sensing system covalently bound to the oxidized NC*

The possibility of attaching covalently GOx to the test-strip was also explored herein, aiming to increase the stability of the final device. This was made by employing NHS/EDC chemistry. In this, the carboxylate groups in the carboxyl- NC matrix were activated and underwent subsequent covalent binding to the amine groups exposed in the outer surface of GOx. The concentration of GOx bound to the activated carboxylic groups ranged from 0.01 to 20 mg/mL.

The results obtained are shown in Fig. 6. Comparing with the

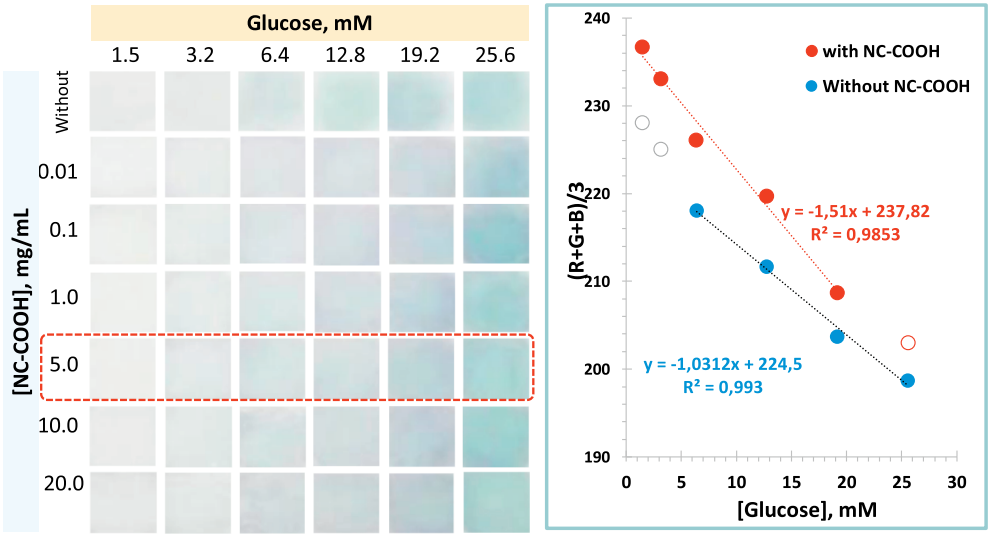

Fig. 5. Digital images of the test-strips in the presence of different glucose concentrations using ABTS as colorimetric indicator, prepared with different concentrations of carboxyl- NC (left) and the analytical calibration curves plotting the colour coordinates collected against the glucose concentration (right, the carboxyl-NC assay corresponds to 5 mg/mL of NC-COOH).

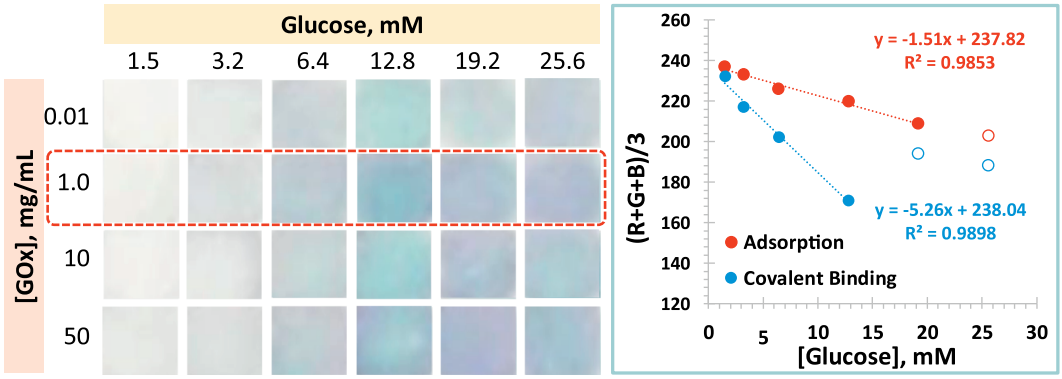

Fig. 6. Digital images of the test-strips in the presence of different glucose concentrations using ABTS as colorimetric indicator, prepared with different concentrations of GOx covalently bound (left) and the analytical calibration curves plotting the colour coordinates collected against the glucose concentration (right, the carboxyl- NC assay corresponds to 1 mg/mL GOx).

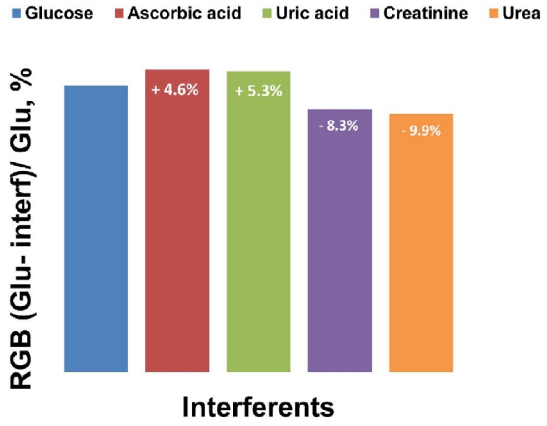

Fig. 7. Evaluation of interfering species variation in comparison with glucose.

adsorption assay, covalent immobilization showed much more intense colours that lead to much more sensitive readings. The slope of the 3.5-times higher, increasing from 1.5 to 5.3 a.u/mM. As expected, this increase in insensitivity was also linked to a narrower concentration range of linear response, ranging from 1.5 and 12.8 mM.

Overall, the method described herein is an expeditious and low cost approach that may be further explored in the analysis of glucose in urine. Normal levels may reach up to 150 mg/L, meaning that normal urine samples may require 10× dilution prior to analysis with the test-strip. Moreover, urine samples shall not have intrinsic colour that may interfere with this determination.

3.5. Selectivity assay

Ascorbic acid, uric acid, creatinine and urea were incubated onto the paper substrate simultaneously with glucose and compared with glucose incubated alone. It can be seen in Fig. 7 that the response of the paper test-strip was not affected by other interferents as the variation of the tested interfering species is low (less than 10%) comparing to glucose value. Ascorbic acid and uric acid showed a slightly positive variation whereas creatinine and urea revealed a low negative variation, over the glucose value.

4. Conclusions

This work reports the oxidative modification of MCC to generate water-soluble cellulose derivatives that may enhance the use of test-strips making use of cellulose substrates as support. Different conditions were applied herein. Overall, it was possible to reach better properties of the cellulose substrate material by using a suitable ratio of TEMPO/hypochlorite and an appropriate number of consecutive oxidative procedures.

The use of carboxyl- NC to improve cellulose substrates to which enzyme binding is required was further tested. It was shown that modified NC showed better colour distribution and improved the process of glucose detection in terms of analytical performance.

Overall, the proposed enzymatic test-strip showed good features in terms of simplicity, response time, price, disposability, being a promising tool for point-of-care analysis. Moreover, this device opens horizons for multiplex purposes by using different chromogenic reagents. It may be further extended to the detection of a broad kind of analytes of interest in food, health and environmental applications, by using the inherent capability in H_2O_2-producing oxidases.

Declaration of Competing Interest

The authors declare that they have no known competing financial interests or personal relationships that could have appeared to influence the work reported in this paper.

Acknowledgments

The Portuguese Science and Technology Foundation, I.P. (FCT), is acknowledged for the financial support through the project reference P2020-PTDC/AAG-TEC/5400/2014 (also POCI-01-0145-FEDER-016637, FEDER, COMPETE, POCI) and POCTEP/INTERREG is also acknowledged through the project 2QBioneuro, Impulso de una red de I+i en química biológica para diagnóstico y tratamiento de enfermedades neurológicas. MCCGC acknowledges FCT for the PhD grant SFRH/BD/131959/2017. The Portuguese Foundation for Science and Technology (FCT) under the scope of the strategic funding of UIDB/04469/2020 unit and BioTecNorte operation (NORTE-01-0145-FEDER-000004) funded by the European Regional Development Fund under the scope of Norte2020 - Programa Operacional Regional do Norte.

Appendix A. Supplementary data

Supplementary data to this article can be found online at https://doi.org/10.1016/j.sbsr.2020.100368.

References

[1] G. Siqueira, J. Bras, A. Dufresne, Cellulosic bionanocomposites: a review of preparation, properties and applications, Polymers 2 (2010) 728–765.
[2] X. Guo, L. Liu, Y.C. Hu, Y.Q. Wu, Water vapor sorption properties of TEMPO oxidized and sulfuric acid treated cellulose nanocrystal films, Carbohydr. Polym. 197 (2018) 524–530.
[3] D. Hoenders, J.Q. Guo, A.S. Goldmann, C. Barner-Kowollik, A. Walther,

Photochemical ligation meets nanocellulose: a versatile platform for self-reporting functional materials, Mater. Horizons 5 (2018) 560–568.
[4] C. Zhuang, F.R. Tao, Y.Z. Cui, Eco-friendly biorefractory films of gelatin and TEMPO-oxidized cellulose ester for food packaging application, J. Sci. Food Agric. 97 (2017) 3384–3395.
[5] M. Haniffa, Y.C. Ching, C.H. Chuah, K.Y. Ching, N. Nazri, L.C. Abdullah, L. Nai-Shang, Effect of TEMPO-oxidization and rapid cooling on thermo-structural properties of nanocellulose, Carbohydr. Polym. 173 (2017) 91–99.
[6] H. Golmohammadi, E. Morales-Narvaez, T. Naghdi, A. Merkoci, Nanocellulose in sensing and biosensing, Chem. Mater. 29 (2017) 5426–5446.
[7] J. George, S.N. Sabapathi, Cellulose nanocrystals: synthesis, functional properties, and applications, Nanotechnol. Sci. Appl. 8 (2015) 45–54.
[8] M. Samir, F. Alloin, A. Dufresne, Review of recent research into cellulosic whiskers, their properties and their application in nanocomposite field, Biomacromolecules 6 (2005) 612–626.
[9] M.M.D. Lima, R. Borsali, Rodlike cellulose microcrystals: structure, properties, and applications, Macromol. Rapid Commun. 25 (2004) 771–787.
[10] J. Sugiyama, R. Vuong, H. Chanzy, Electron-diffraction study on the 2 crystalline phases occurring in native cellulose from an algal cell-wall, Macromolecules 24 (1991) 4168–4175.
[11] W. Helbert, Y. Nishiyama, T. Okano, J. Sugiyama, Molecular imaging of Halocynthia papillosa cellulose, J. Struct. Biol. 124 (1998) 42–50.
[12] M.M. Mahmud, A. Perveen, R.A. Jahan, M.A. Matin, S.Y. Wong, X. Li, M.T. Arafat, Preparation of different polymorphs of cellulose from different acid hydrolysis medium, Int. J. Biol. Macromol. 130 (2019) 969–976.
[13] I. Shahabi-Ghahafarrokhi, F. Khodaiyan, M. Mousavi, H. Yousefi, Preparation and characterization of nanocellulose from beer industrial residues using acid hydrolysis/ultrasound, Fibers Polym. 16 (2015) 529–536.
[14] H.X. Xie, H.S. Du, X.G. Yang, C.L. Si, Recent strategies in preparation of cellulose nanocrystals and cellulose nanofibrils derived from raw cellulose materials, Int. J. Polym. Sci. 2918 (2018) 25. Article ID 7923068.
[15] N. Hastuti, K. Kanomata, T. Kitaoka, Hydrochloric acid hydrolysis of pulps from oil palm empty fruit bunches to produce cellulose nanocrystals, J. Polym. Environ. 26 (2018) 3698–3709.
[16] J. Araki, M. Wada, S. Kuga, Steric stabilization of a cellulose microcrystal suspension by poly(ethylene glycol) grafting, Langmuir 17 (2001) 21–27.
[17] Y. Habibi, H. Chanzy, M.R. Vignon, TEMPO-mediated surface oxidation of cellulose whiskers, Cellulose 13 (2006) 679–687.
[18] L. Li, S. Zhao, J. Zhang, Z.X. Zhang, H.Q. Hu, Z.X. Xin, J.K. Kim, TEMPO-mediated oxidation of microcrystalline cellulose: influence of temperature and oxidation procedure on yields of water-soluble products and crystal structures of water-insoluble residues, Fibers Polym. 14 (2013) 352–357.
[19] D.D. Perez, S. Montanari, M.R. Vignon, TEMPO-mediated oxidation of cellulose III, Biomacromolecules 4 (2003) 1417–1425.
[20] A.E.J. Denooy, A.C. Besemer, H. Vanbekkum, Highly selective tempo mediated oxidation of primary alcohol groups in polysaccharides, J. R. Netherlands Chem. Soc. 113 (1994) 165–166.
[21] A. Isogai, Y. Kato, Preparation of polyglucuronic acid from cellulose by TEMPO-mediated oxidation, Cellulose 5 (1998) 153–164.
[22] C. Tahiri, M.R. Vignon, TEMPO-oxidation of cellulose: synthesis and characterisation of polyglucuronans, Cellulose 7 (2000) 177–188.
[23] T. Saito, A. Isogai, TEMPO-mediated oxidation of native cellulose. The effect of oxidation conditions on chemical and crystal structures of the water-insoluble fractions, Biomacromolecules 5 (2004) 1983–1989.
[24] T. Saito, I. Shibata, A. Isogai, N. Suguri, N. Sumikawa, Distribution of carboxylate groups introduced into cotton linters by the TEMPO-mediated oxidation, Carbohydr. Polym. 61 (2005) 414–419.
[25] S. Montanari, M. Rountani, L. Heux, M.R. Vignon, Topochemistry of carboxylated cellulose nanocrystals resulting from TEMPO-mediated oxidation, Macromolecules 38 (2005) 1665–1671.
[26] M. Portaccio, D. Durante, A. Viggiano, S. Di Martino, P. De Luca, D. Di Tuoro, U. Bencivenga, S. Rossi, P. Canciglia, B. De Luca, D.G. Mita, Amperometric glucose determination by means of glucose oxidase immobilized on a cellulose acetate film: dependence on the immobilization procedures, Electroanalysis 19 (2007) 1787–1793.
[27] A.P.M. Tavares, N.S. Ferreira, L. Truta, M.G.F. Sales, Conductive paper with antibody-like film for electrical readings of biomolecules, Sci. Rep. 6 (2016).
[28] V. Incani, C. Danumah, Y. Boluk, Nanocomposites of nanocrystalline cellulose for enzyme immobilization, Cellulose 20 (2013) 191–200.
[29] E. Morales-Narvaez, H. Golmohammadi, T. Naghdi, H. Yousefi, U. Kostiv, D. Horak, N. Pourreza, A. Merkoci, Nanopaper as an optical sensing platform, ACS Nano 9 (2015) 7296–7305.
[30] M. Tavakolian, J. Lerner, F.M. Tovar, J. Frances, T.G.M. van de Ven, A. Kakkar, Dendrimer directed assembly of dicarboxylated hairy nanocellulose, J. Colloid Interface Sci. 541 (2019) 444–453.
[31] K.M.A. Uddin, V. Jokinen, F. Ahangiri, S. Franssila, O.J. Rojas, S. Tuukkanen, Disposable microfluidic sensor based on nanocellulose for glucose detection, Global Chall. 3 (2019).
[32] H.B. Yuan, L. Chen, F.F. Hong, M.F. Zhu, Evaluation of nanocellulose carriers produced by four different bacterial strains for laccase immobilization, Carbohydr. Polym. 196 (2018) 457–464.
[33] Y. Potzinger, L. Rahnfeld, D. Kralisch, D. Fischer, Immobilization of plasmids in bacterial nanocellulose as gene activated matrix, Carbohydr. Polym. 209 (2019) 62–73.
[34] Y.M. Xiao, L.D. Rong, B.J. Wang, Z.P. Mao, H. Xu, Y. Zhong, L.P. Zhang, X.F. Sui, A light-weight and high-efficacy antibacterial nanocellulose-based sponge via covalent immobilization of gentamicin, Carbohydr. Polym. 200 (2018) 595–601.
[35] W.T. Wulandari, A. Rochliadi, I.M. Arcana, Iop, nanocellulose prepared by acid hydrolysis of isolated cellulose from sugarcane bagasse, 10th Joint Conference on ChemistrySolo, Indonesia, 2015.
[36] M.M. Abdi, R.L. Razalli, P.M. Tahir, N. Chaibakhsh, M. Hassani, M. Mir, Optimized fabrication of newly cholesterol biosensor based on nanocellulose, Int. J. Biol. Macromol. 126 (2019) 1213–1222.
[37] H. Gomes, M.G.F. Sales, Development of paper-based color test-strip for drug detection in aquatic environment: application to oxytetracycline, Biosens. Bioelectron. 65 (2015) 54–61.
[38] M. Sher, R. Zhuang, U. Demirci, W. Asghar, Paper-based analytical devices for clinical diagnosis: recent advances in the fabrication techniques and sensing mechanisms, Expert. Rev. Mol. Diagn. 17 (2017) 351–366.
[39] J. Hu, S.Q. Wang, L. Wang, F. Li, B. Pingguan-Murphy, T.J. Lu, F. Xu, Advances in paper-based point-of-care diagnostics, Biosens. Bioelectron. 54 (2014) 585–597.
[40] G.A. Posthuma-Trumpie, J. Korf, A. van Amerongen, Lateral flow (immuno) assay: its strengths, weaknesses, opportunities and threats. A literature survey, Anal. Bioanal. Chem. 393 (2009) 569–582.
[41] C. Carrell, A. Kava, M. Nguyen, R. Menger, Z. Munshi, Z. Call, M. Nussbaum, C. Henry, Beyond the lateral flow assay: a review of paper-based microfluidics, Microelectron. Eng. 206 (2019) 45–54.
[42] J. Dyerberg, L. Pedersen, O. Aagaard, Evaluation of a dipstick test for glucose in urine, Clin. Chem. 22 (1976) 205–210.
[43] R. Hamilton, S. Young, Identifying CSF using urine glucose dipstick testing, Int. J. Obstet. Anesth. 16 (2007) 294–295.
[44] E.T. Bushman, V.C. Jauk, J.M. Szychowski, S. Mazzoni, A.T. Tita, L.M. Harper, Utility of routine dipstick urinalysis for glucose screening as a predictor for gestational diabetes, Am. J. Obstet. Gynecol. 222 (2020) S161–S162.
[45] J.H. Kim, S. Mun, H.U. Ko, G.Y. Yun, J. Kim, Disposable chemical sensors and biosensors made on cellulose paper, Nanotechnology 25 (2014).
[46] C. Fischer, A. Fraiwan, S. Choi, A 3D paper-based enzymatic fuel cell for self-powered, low-cost glucose monitoring, Biosens. Bioelectron. 79 (2016) 193–197.
[47] J.D. Newman, S.J. Setford, Enzymatic biosensors, Mol. Biotechnol. 32 (2006) 249–268.
[48] A. Sassolas, L.J. Blum, B.D. Leca-Bouvier, Immobilization strategies to develop enzymatic biosensors, Biotechnol. Adv. 30 (2012) 489–511.
[49] F.T.C. Moreira, M.G.F. Sale, M. Di Lorenzo, Towards timely Alzheimer diagnosis: a self-powered amperometric biosensor for the neurotransmitter acetylcholine, Biosens. Bioelectron. 87 (2017) 607–614.
[50] H.H. Nguyen, S.H. Lee, U.J. Lee, C.D. Fermin, M. Kim, Immobilized enzymes in biosensor applications, Materials 12 (2019).
[51] G.Y. Dai, J.L. Hu, X.Y. Zhao, P. Wang, A colorimetric paper sensor for lactate assay using a cellulose-binding recombinant enzyme, Sens. Actuat. B 238 (2017) 138–144.
[52] F. Derikvand, D.T. Yin, R. Barrett, H. Brumer, Cellulose-based biosensors for esterase detection, Anal. Chem. 88 (2016) 2989–2993.
[53] S. Palanisamy, S.K. Ramaraj, S.M. Chen, T.C.K. Yang, P. Yi-Fan, T.W. Chen, V. Velusamy, S. Selvam, A novel laccase biosensor based on laccase immobilized graphene-cellulose microfiber composite modified screen-printed carbon electrode for sensitive determination of catechol, Sci. Rep. 7 (2017).
[54] M. Arciuli, G. Palazzo, A. Gallone, A. Mallardi, Bioactive paper platform for colorimetric phenols detection, Sens. Actuat. B 186 (2013) 557–562.
[55] Y. Liu, J.Y. Chen, Enzyme immobilization on cellulose matrixes, J. Bioact. Compat. Polym. 31 (2016) 553–567.
[56] C.S.K. Lawrence, S.N. Tan, C.Z. Floresca, A "green" cellulose paper based glucose amperometric biosensor, Sens. Actuat. B 193 (2014) 536–541.
[57] A. Bohm, S. Trosien, O. Avrutina, H. Kolmar, M. Biesalski, Covalent attachment of enzymes to paper fibers for paper-based analytical devices, Front. Chem. 6 (2018).
[58] N.S. Firooz, R. Panahi, B. Mokhtarani, F. Yazdani, Direct introduction of amine groups into cellulosic paper for covalent immobilization of tyrosinase: support characterization and enzyme properties, Cellulose 24 (2017) 1407–1416.
[59] M. Zhou, M.H. Yang, F.M. Zhou, Paper based colorimetric biosensing platform utilizing cross-linked siloxane as probe, Biosens. Bioelectron. 55 (2014) 39–43.
[60] M.P. Guerrero, F. Bertrand, D. Rochefort, Activity, stability and inhibition of a bioactive paper prepared by large-scale coating of laccase microcapsules, Chem. Eng. Sci. 66 (2011) 5313–5320.
[61] J.J. Wang, N.V. Myung, M.H. Yun, H.G. Monbouquette, Glucose oxidase entrapped in polypyrrole on high-surface-area Pt electrodes: a model platform for sensitive electroenzymatic biosensors, J. Electroanal. Chem. 575 (2005) 139–146.
[62] M.F. Rosa, E.S. Medeiros, J.A. Malmonge, K.S. Gregorski, D.F. Wood, L.H.C. Mattoso, G. Glenn, W.J. Orts, S.H. Imam, Cellulose nanowhiskers from coconut husk fibers: effect of preparation conditions on their thermal and morphological behavior, Carbohydr. Polym. 81 (2010) 83–92.
[63] Q.Q. Wang, J.Y. Zhu, R.S. Reiner, S.P. Verrill, U. Baxa, S.E. McNeil, Approaching zero cellulose loss in cellulose nanocrystal (CNC) production: recovery and characterization of cellulosic solid residues (CSR) and CNC, Cellulose 19 (2012) 2033–2047.
[64] K. Nie, Y. Song, S.Y. Liu, G.T. Han, H.X. Ben, A.J. Ragauskas, W. Jiang, Preparation and characterization of microcellulose and nanocellulose fibers from *Artemisia vulgaris* bast, Polymers 11 (2019).